

THE INTERNATIONAL JOURNAL OF SCIENCE & TECHNOLEDGE

Effects of Varying Spray Pyrolysis Parameters on the Microstructure of Solid Oxide Fuel Cell Cathodes

Obasi, B. I.

Senior Lecturer, Department of Physics/Electronics, Federal Polytechnic, Nekede, Owerri, Nigeria

Omenikolo, A. I.

Senior Lecturer, Department of Physics/Electronics, Federal Polytechnic, Nekede, Owerri, Nigeria

Agbakwuru, B. C.

Lecturer, Department of Physics/Electronics, Federal Polytechnic, Nekede, Owerri, Nigeria

Okoro, U. C.

PG Student, Department of Physics Michael Okpara University of Agriculture, Umudike, Nigeria

Abstract:

Recent studies in solid oxide fuel cells (SOFC), targets the reduction of operating temperature as well as retaining maximum power output and reduced cost. A promising strategy is in the deposition of gradient porous cathode for use in SOFC at lower temperature. This work is directed at studying the effects on surface morphology, film homogeneity and porosity of lanthanum strontium manganite (LSM) on changing the precursor concentration, nozzle-to-substrate distance, deposition temperature, and solution flow rate. The films crystalline phases, surface morphology and composition, were characterized with the x-ray diffractometer, scanning electron microscope (SEM) and energy dispersive spectroscopy (EDS). The investigation revealed variations in the microstructure from dense to more porous LSM films at varying temperatures ranging from 300 to 500°C, a solution flow rate in the range of 0.6 - 1.1ml/min, precursor concentration between 0.1 – 0.5M. The crystal analysis revealed phase change from cubic to rhombohedral structure on annealing of the deposited film.

Keyword: Fuel cell, microstructure, lanthanum strontium manganite, flow rate, scanning electron microscopy, morphology

1. Introduction

Global warming consequences have led the desire for decreasing dependence on hydrocarbon supplies and have led action towards rapid development of alternative high efficiency energy technologies. These have resulted to the development and commercialization of electrochemical energy storage like batteries and fuel cells. Fuel cells have shown to be promising alternative resources in efficient and low emission power generation. Fuel cells are the electrochemical engines that convert the chemical energy from a fuel into electricity through a chemical reaction of positively charged hydrogen ions with oxygen or another oxidizing agent with high efficiency and low pollution (Khurmi and Sedha, 2014; Cha *et al.*, 2006). Moreover, the waste heat from fuel cell can boost the entire system efficiency and at the same time, pure water can be extracted from the process. Fuelcell are classified, based on the electrolyte material, the substance that transports the ions. The electrolyte dictates the operating temperature of a fuel cell type. The principal types include the alkaline fuel cell (AFC), proton exchange membrane (PEM) fuel cell, direct methanol fuel cell (DMFC), molten carbonate fuel cell (MCFC), phosphoric acid fuel cell (PAFC) and solid oxide fuel cell (SOFC). According to Carton *et al.* (2012), proton-exchange membrane (PEM) and solid oxide, fuel cells (SOFC) with all solid components are currently the most attracting technologies for automotive and stationary applications due to their potential for higher power and energy densities amongst fuel cells. Solid oxide fuel cells (SOFC) are solid-electrolyte type of fuel cells that uses Yttrium stabilized Zirconia (YSZ) as the electrolyte. SOFC are economical compared to other fuel cells because it possesses the highest power density in the range of 0.15 – 0.7Wcm⁻², fuel flexibility, variability of cell arrangement and non-requirement of expensive metal catalysts. These advantages are restrained by high operating temperature (600 – 1000°C), and the ceramic nature of all component parts of the SOFC possess some major tasks towards commercialization of the technology. Cost and durability are the main challenges in SOFC structure for the entire range of possible applications (Yamamoto, 2000; Ormerod, 2003). One suggested solution is reducing the operating temperature SOFC to intermediate temperature (500 – 750°C) that will allow the use of cheaper materials in the entire cell and increasing life span of the technology. However, moving to lower operating temperatures is the basis of some critical difficulties in functionality of the cell components (Steele, 2000; Zuo *et al.*, 2006).

Lanthanum strontium manganite (LSM), is considered as one of the most promising cathode materials for SOFC due to its high thermal and chemical stability particularly with YSZ electrolyte (Neumann, *et al.*, 2012).The main problem arises when lowering the temperature results in increasing polarization resistance between LSM cathode and YSZ electrolyte (Sun *et al.*, 2008; Fu *et al.*, 2007).

Recent studies have shown the potential of $\text{GdBaCo}_2\text{O}_{5+\delta}$ and $\text{SmBaCo}_2\text{O}_{5+x}$ with layered and double-layered structures, respectively for operations at reduced temperature due to low activation energy (Xia *et al.*, 2016; Zhang *et al.*, 2008). Although, some properties may mark undesirable changes while others will improve using this trend. Lanthanum strontium cobaltite (LSC) shows electrical and ionic conductivity at low temperature compared to LSM, however its thermal coefficient of expansion is much higher than those of typical SOFC electrolyte (Sun *et al.*, 2008).

Advanced fabrication techniques, to improve the microstructures that compensates for issues that would result in performance losses due to low operating temperature are available. These techniques have established range of advantages over other method (Iwai *et al.*, 2010). However, processing techniques that are capable of cost effective and large-scale manufacturing of functional, porous and nanostructured electrode with improved properties have being attempted (Hamedani *et al.*, 2009; Li *et al.*, 2006). The cathode microstructure is one of the very important parameters determining SOFC performance, since the thermal stability and electrochemical performance of SOFC depends on its chemical composition, microstructure and morphology of the electrode. Therefore, graded electrode structure with a finer microstructure with porosity close to the electrolyte and coarser microstructure with larger porosity away from it has to be developed (Shearing *et al.*, 2010; Gostović, 2009; Gong *et al.*, 2006).

Functionally graded material approach has been applied to SOFC components to combine benefits of compositional and microstructural differences like porosity in some spatial direction into components design to increase the functionality of individual layers at low temperatures (Greene *et al.*, 2006). It is of interest that grading will reduce the thermal coefficient of expansion mismatch between the electrode and the electrolyte resulting in improved adhesion, durability and mechanical stability of the cell components. In review of the work towards studying the effect on the microstructure and morphology of the LSM film by changing deposition parameters (Lintanf *et al.*, 2008; Hamedani *et al.*, 2008; Marinha *et al.*, 2009), acryalline graded permeable LSM cathode was prepared for use in intermediate temperature SOFC by improving the preparation parameters by varying the solvent, temperature and rate of solution flow.

2. Materials and Method

Spray pyrolysis, was used in this work for the deposition. The solution is prepared by dissolving the stoichiometric ratios of the desired precursor into solvent using a magnetic stirring. The average spray time for deposition of a 50ml solution was between 30 – 45 minutes depending on the spray conditions. Thereafter, cooling of the sample from the deposition temperature to room temperature occurred at the rate of 5°C/min to 10°C/min.

2.1. Deposition of LSM Cathode

YSZ electrolyte substrates were prepared by compacting 8mol of yttria stabilized zirconia powders into pellet of 0.025m in diameter and thickness of about 0.001m using a hydrostatic press. To make a dense electrolyte substrate, the pellets were heated to a temperature of 1400°C, at the rate of 4°C/min, held for 1 hour and then cooled to room temperature at the same rate of 4°C/min. The LSM solution was prepared from dissolving $\text{La}(\text{TMHD})_3$, $\text{Sr}(\text{TMHD})_2$ and $\text{Mn}(\text{TMHD})_3$ as the precursors of La, Sr and Mn into dimethylglycol at the ratios of 0.8:0.2: 1 in that order and then sprayed to the YSZ substrate at 500°C with the oxygen and nitrogen gas flow of 80 and 800ml/min respectively. The nozzle to substrate distance was constant at all time during any stage of the experiment. The samples were annealed at 750°C for 4 hours and allowed to cool to room temperature. Spray pyrolysis in various speed-temperature spray phases, were performed to obtain the deposition of a graded porous LSM cathode on the YSZ substrate.

2.2. Characterization Techniques

The samples were characterized by using a FEI Nova Nano scanning electron microscopes (SEM) for the morphology, pore sizes, structure and distribution, surface and 3-D cross sectional structure and microstructure changes with changing deposition parameters. The analysis of the chemical composition of a sample was by the energy dispersive X-ray spectroscopy (EDS). The identification of the crystalline phase of the materials was by the x-ray diffraction based on the Bragg's law.

3. Results and Discussions

Figure 1 depicts the crystalline phase analysis of the sample before and after annealing. The peak indicates cubic YSZ substrate and rhombohedral phase of LSM before and after annealing. The sharp peaks in the XRD patterns are apparently due to the LSM film non-amorphous formation. The sharp peaks also indicate increase of crystallinity after annealing. Overall, the samples indicate a slightly porous microstructure resulting from very low deposition temperature.

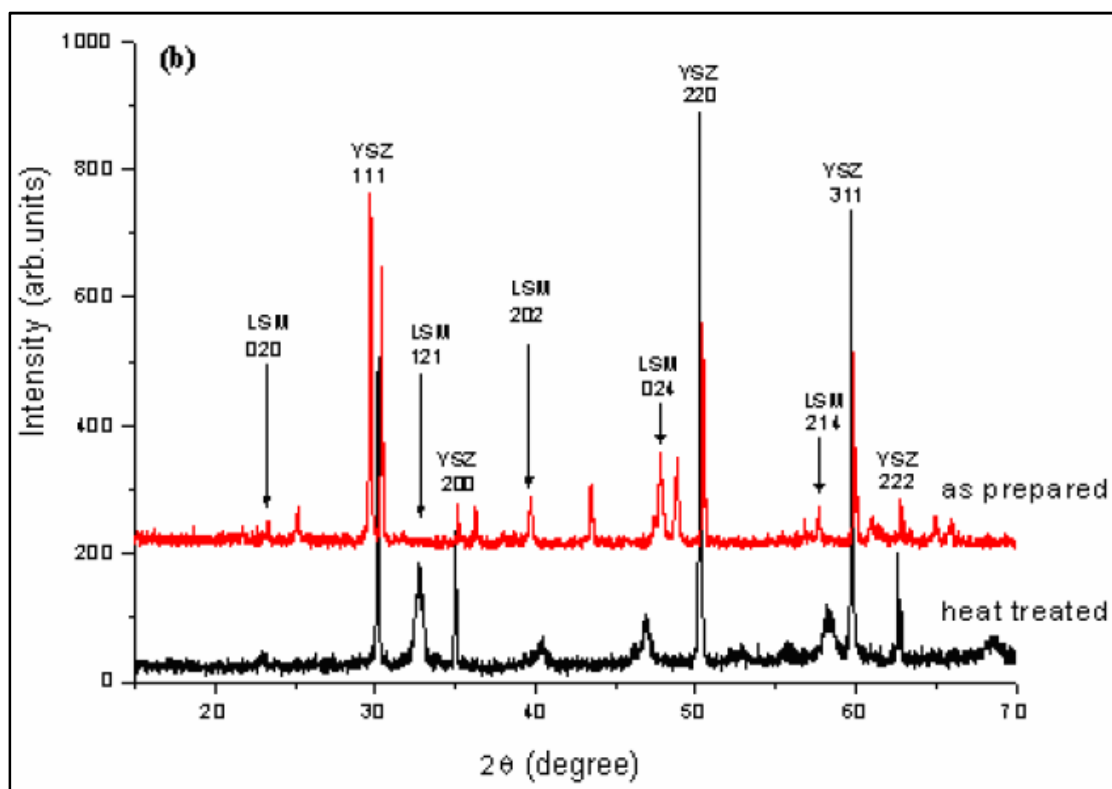


Figure 1: The XRD spectra of samples before and after annealing

Figure 2 shows SEM micrograph microstructures and cross section of the LSM cathode film deposited on a YSZ substrate before and after annealing. The sample did not reveal surface crack as shown in Figures 1.2(a) before annealing and (b) after annealing. This may be due to the small temperature difference between sprayed cathode and the YSZ surface. Examination of the film thickness, from the cross sections shown in Fig. 1.3(a) and (b) reveals that the microstructure did not present many changes before annealing and after annealing. Chemical analysis of the sample with EDS showed that the composition is not homogeneous throughout the film. The EDS data obtained from various points on the sample exposed stoichiometry ratios, La: Sr: Mn = 0.8:0.2:1 after annealing.

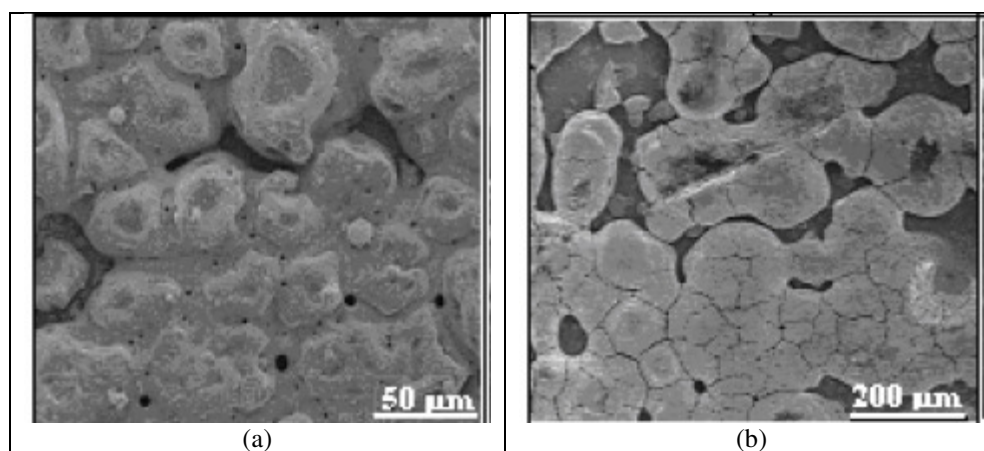


Figure 2: SEM micrograph of the LSM film (a) before annealing and (b) after annealing.

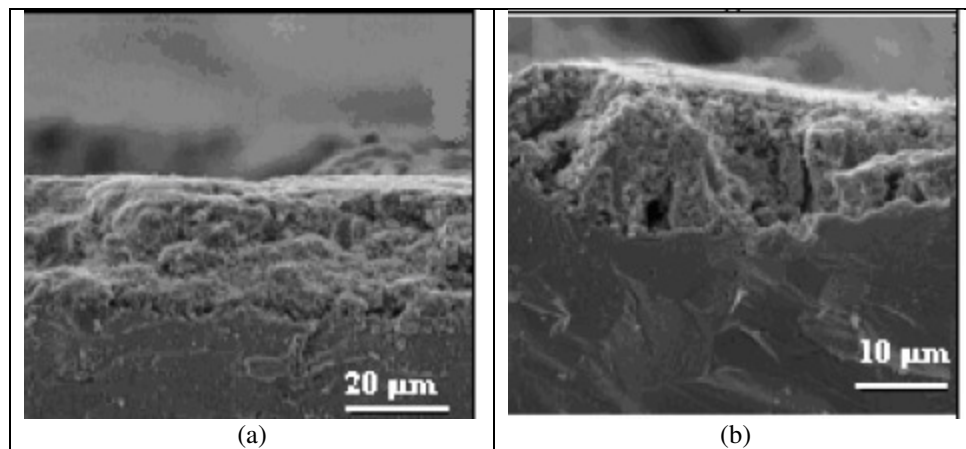


Figure 3: Cross section of the LSM film (a) before annealing and (b) after annealing

3.1. Effects of Varying Temperature of the LSM Film

Figure 4 depicts the effect of deposition temperature on LSM microstructure. The figure reveals the SEM cross sections of the samples for varying deposition temperatures. At deposition temperatures of 300°C (Fig. 14), the resulting film structure included large circles of the solid amorphous regions, embedded uniformly over the surface. Fig. 1.4(b) depicts the SEM at temperature of 400°C observation showed pore growth and formation of doughnut-shape features within the film. Observations at temperatures of 500 °C revealed the formation of identical dense layers as shown in Figure 4(c). Observation revealed that the most significant changes in microstructure were at higher temperatures because at higher deposition temperatures the precursors decompose leading to the formation of very porous film. Hence, varying temperature mostly affects film porosity and morphology.

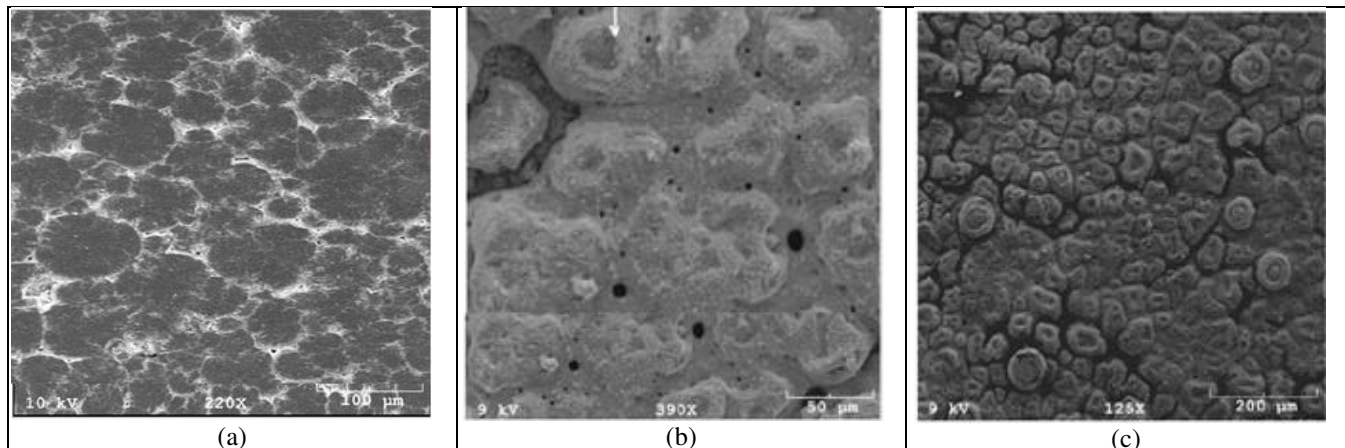


Figure 4: SEM micrograph of the LSM film deposited at temperatures of (a) 300°C (b) 400°C and (c) 500°C.

3.2. Effect of Solution Flow Rate

Figure 5 and Figure 6 show the effect of solution flow rate from 0.6, 1.1 and 1.6 ml/min on the microstructure of the LSM film deposited at 500°C and 600°C respectively. At 500°C temperature, the film deposited using solution flow rate of 0.6ml/min looks powdery as observed in Figures 1.5(a) compared to the films deposited at solution flow rates of 1.1ml/min (Figure 5(b)). At a solution flow rate, of 1.6ml/min (Figure 5(c)) leads to formation of much thinner layers. Further, investigation showed that increasing the solution flow rate at high temperatures led to a more agglomerated porous structure as shown in Figure 6(a) to (c). This is because of high activation energy that will take less time for the droplet to spread over the substrate. Therefore, the solution flow rate is an important factor in controlling the microstructure of the LSM film deposited.

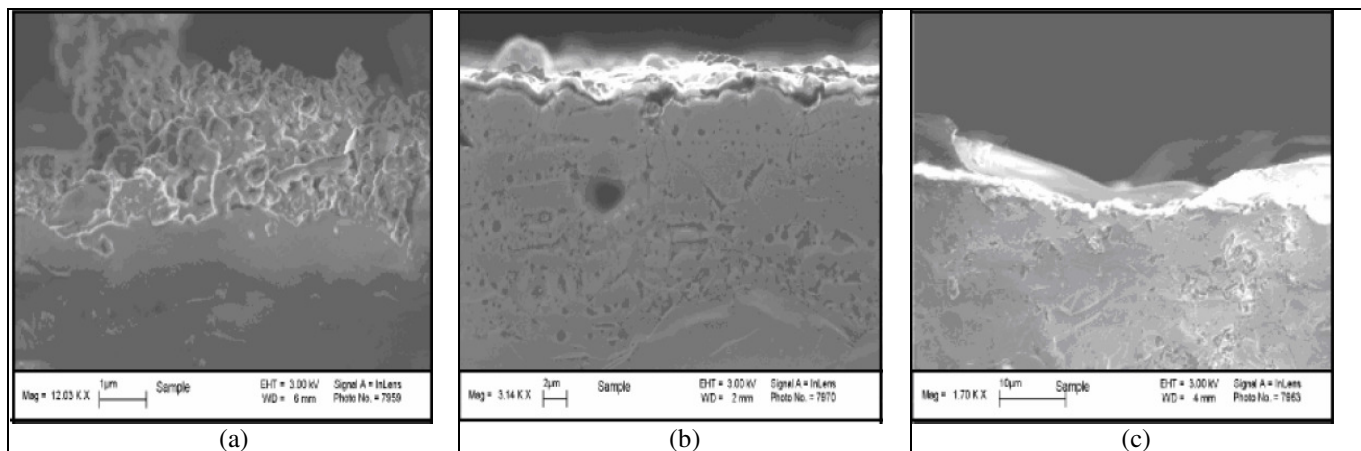


Figure 5: The effect of the solution flow rate on the microstructure of the LSM film deposited at 500°C at the flow rate of 0.6, 1.1 and 1.6ml/min respectively

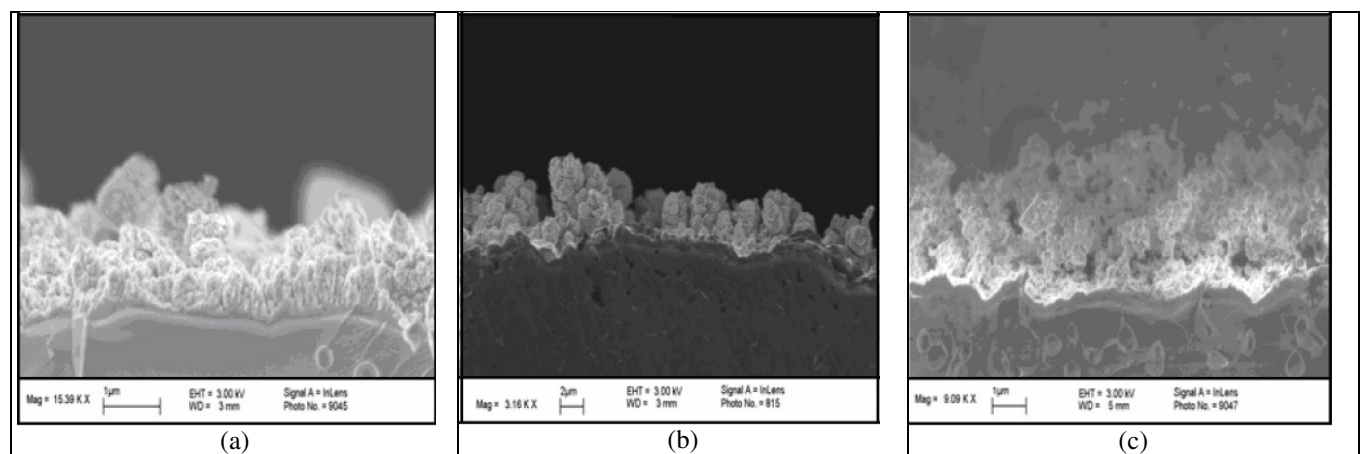


Figure 6: The effect of the solution flow rate on the microstructure of the LSM film deposited at 600°C at the flow rate of 0.6, 1.1 and 1.6ml/min respectively

3.3. Effect of Nozzle-to-Substrate Distance

Figure 7 depicts the effect of nozzle-to-substrate distance on LSM microstructure. The distance between the spray nozzle and the substrate was varied within the range of 0.035m to 0.085m while the deposition, temperature and solution flow rate were kept constant at 500°C and 1.1ml/min respectively. At the distance of 0.035m, the film formed was dense. At a distance of 0.065m, the films formed were thin and dispersed on the surface of the substrate and tend to form powder. Moreover, at a distance of 0.85m, only a small portion of droplets can reach the surface of the substrate and therefore the spray efficiency is small. The effects of varying nozzle-to-substrate distance on the surface morphology of the films produced did not appear to be critical.

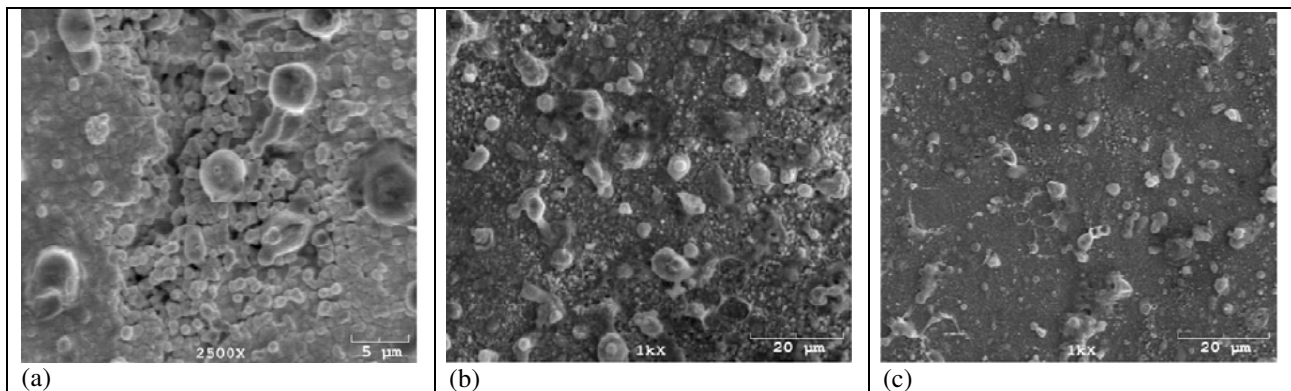


Figure 7: Effect of nozzle-to-substrate distance on the microstructure of the LSM film, (a) 0.035m, (b) 0.065m and 0.085m.

3.4. Effect of Precursor Concentration

The size and morphology of particles in the films showed to be dependent on the solution concentration while all the other parameters are constant. The effect of changing the solution concentration results in changing the particle size. Observation showed significant changes at the extremes of solution concentration by varying the solution concentration of Mn from 0.1M to 0.5M. Observation showed that particles formed were large with a high degree of cluster at concentration of 0.05M, while there was formation of small particles at concentration of 0.1M as shown in Figure 8. The films were more porous at high concentration, due to the formation of large particles with a high degree of cluster. At low concentrations, the film formed a dense layer with particles that were implanted orderly on the surface. According to Obasi *et al.* (2016), thin films appear to be more homogenous with decreasing concentration.

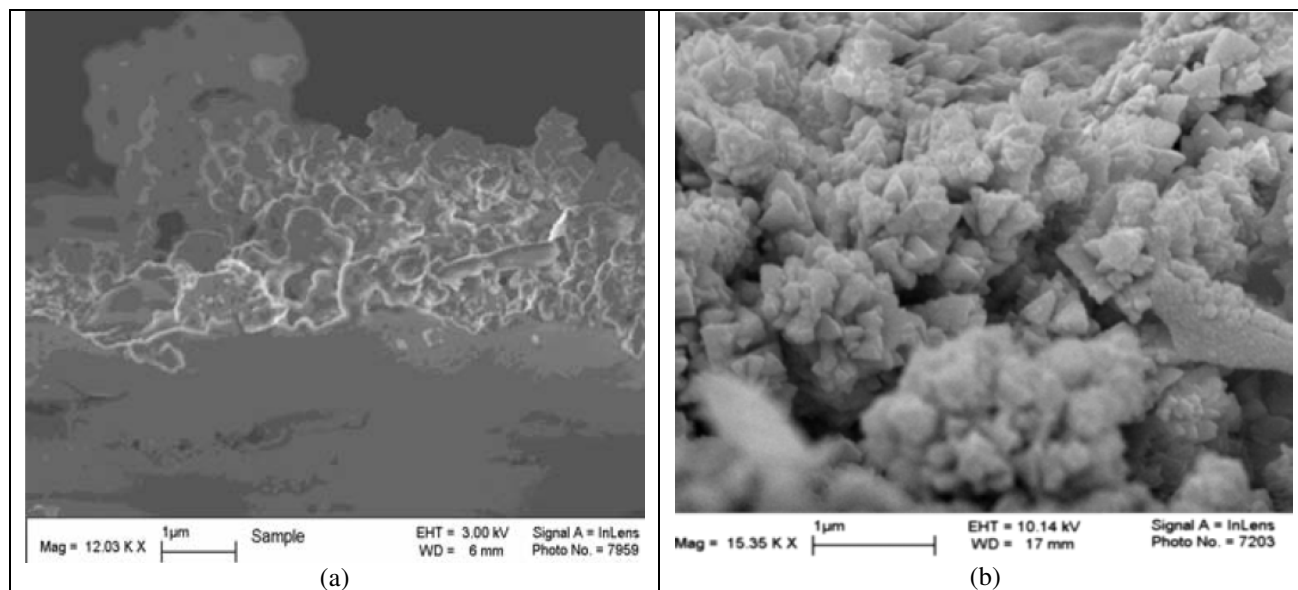


Figure 8: SEM cross sections of the LSM film deposited from (a) high and (b) low concentration precursor solutions at 500°C.

4. Conclusion

Spray pyrolysis techniques was used for the deposition of cathodes microstructure resulting to a variety of morphologies and porosity. The result presented a homogeneous crack free deposition. The report presenting the investigation of the effect of temperature of deposition, solution flow rate, nozzle-to-substrate distance and precursor concentration on the morphology and microstructure of LSM thin film. It was evident that the temperature of deposition, the solution flow rate along and the solution concentration are responsible for the characteristics of the deposited film. Control of the morphology and porosity of the microstructure of the films was based on the effects of changing the deposition temperature in the range of 300 – 600°C, the solution flow rate from 0.6–1.1ml/min and precursor concentration at 0.1M and 0.5M. Observation showed that the temperature at which the LSM films changed to the Perovskite phase are significantly below the sintering temperature required for traditional methods of the film preparation. Hence, this work brings the possibility of using spray pyrolysis techniques for fabrication of SOFC components with control over microstructure and porosity of the films without requiring post annealing at high temperature.

5. References

- i. Carton, J. G., Lawlor, V., Olabi, A. G., Hochenauer, C., & Zauner, G. (2012). Water droplet accumulation and motion in PEM (Proton Exchange Membrane) fuel cell mini-channels. *Energy*, 39(1), 63-73.
- ii. Cha, S. W., Colella, W., & Prinz, F. B. (2006). *Fuel cell fundamentals* (Vol. 2). New York: John Wiley & Sons.
- iii. Fu, C., Sun, K., Zhang, N., Chen, X., & Zhou, D. (2007). Electrochemical characteristics of LSCF–SDC composite cathode for intermediate temperature SOFC. *Electrochimica Acta*, 52(13), 4589-4594.
- iv. Gong, W., Gopalan, S., & Pal, U. B. (2006). Performance of intermediate temperature (600–800°C) solid oxide fuel cell based on Sr and Mg doped Lanthanum-Gallate electrolyte. *Journal of power sources*, 160(1), 305-315.
- v. Gostović, D. (2009). A multi-length scale approach to correlating solid oxide fuel cell porous cathode microstructure to electrochemical performance (Doctoral dissertation, University of Florida).
- vi. Greene, E. S., Chiu, W. K. S., Medeiros, M. G. (2006). Mass transfer in graded microstructure solid oxide fuel cell electrodes. *Journal of Power Sources*. 161(1), 225-231.
- vii. Hamedani, H. A., Dahmen, K. H., Li, D., Peydaye-Saheli, H., Garmestani, H., & Khaleel, M. (2008). Fabrication of gradient porous LSM cathode by optimizing deposition parameters in ultrasonic spray pyrolysis. *Materials Science and Engineering: B*, 153(1), 1-9.
- viii. Hamedani, H. A., Dahmen, K. H., Li, D., & Garmestani, H. (2009). Effect of spray parameters on the microstructure of lahsrxmno₃ cathode prepared by spray pyrolysis. *Advances in Solid Oxide Fuel Cells IV: Ceramic Engineering and Science Proceedings*, 29, (5), 139.

- ix. Iwai, H., Shikazono, N., Matsui, T., Teshima, H., Kishimoto, M., Kishida, R., & Muroyama, H. (2010). Quantification of SOFC anode microstructure based on dual beam FIB-SEM technique. *Journal of Power Sources*, 195(4), 955-961.
- x. Khurmi, R.S. Sedha, R.S. (2014). *Materials Science*, S. Chand & Company Ltd. 5th edition.
- xi. Li, D., Saheli, G., Khaleel, M., & Garmestani, H. (2006). Microstructure optimization in fuel cell electrodes using materials design. *CMC-Tech Science Press*, 4(1), 31.
- xii. Lintanf, A., Djurado, E., & Vernoux, P. (2008). Pt/YSZ electrochemical catalysts prepared by electrostatic spray deposition for selective catalytic reduction of NO by C₃H₆. *Solid State Ionics*, 178(39), 1998-2008.
- xiii. Marinha, D., Rossignol, C., & Djurado, E. (2009). Influence of electro spraying parameters on the microstructure of La_{0.6}Sr_{0.4}Co_{0.2}F_{0.8}O_{3-δ} films for SOFCs. *Journal of Solid State Chemistry*, 182(7), 1742-1748.
- xiv. Neumann, R. F., Bahiana, M., & Binggeli, N. (2012). Magnetic properties of La_{0.67}Sr_{0.33}MnO₃/BiFeO₃ (001) heterojunctions: Chemically abrupt vs. atomic intermixed interface. *EPL (Europhysics Letters)*, 100(6), 67002.
- xv. Obasi B. I., Osuwa, J. C., & Odu, D. A. (2016). Effects of varying copper (Cu) ion concentration of ternary compound of copper iron sulfide (CuFeS) thin films. *International Journal of Science and Technology*. 5(8), 369-373.
- xvi. Ormerod, R. M. (2003). Solid oxide fuel cells. *Chemical Society Reviews*, 32(1), 17-28.
- xvii. Shearing, P. R., Brett, D. J. L., & Brandon, N. P. (2010). Towards intelligent engineering of SOFC electrodes: a review of advanced microstructural characterisation techniques. *International Materials Reviews*, 55(6), 347-363.
- xviii. Steele, B. C. H. (2000). Appraisal of Ce_{1-y}Gd_yO_{2-y/2} electrolytes for IT-SOFC operation at 500 C. *Solid State Ionics*, 129 (1), 95-110.
- xix. Sun, C., Hui, R., & Roller, J. (2008). Cathode materials for solid oxide fuel cells: a review. *J Solid State Electrochem*, 14(7), 1125-1144.
- xx. Xia, L. N., He, Z. P., Huang, X. W., & Yu, Y. (2016). Synthesis and properties of SmBaCo_{2-x}Ni_xO₅₊ perovskite oxide for IT-SOFC cathodes. *Ceramics International*, 42(1), 1272-1280.
- xxi. Yamamoto, O. (2000). Solid oxide fuel cells: fundamental aspects and prospects. *Electrochimica Acta*, 45(15), 2423-2435.
- xxii. Zhang, K., Ge, L., Ran, R., Shao, Z., & Liu, S. (2008). Synthesis, characterization and evaluation of cation-ordered LnBaCo₂O_{5+δ} as materials of oxygen permeation membranes and cathodes of SOFCs. *Acta Materialia*, 56(17), 4876-4889.
- xxiii. Zuo, C., Zha, S., Liu, M., Hatano, M., & Uchiyama, M. (2006). Ba (Zr_{0.1}Ce_{0.7}Y_{0.2})O_{3-δ} as an Electrolyte for Low-Temperature Solid-Oxide Fuel Cells. *Advanced Materials*, 18(24), 3318-3320.